Modeling Impacts Between a Continuous System and a Rigid Obstacle Using Coefficient of Restitution

Chandrika P. Vyasarayani[1]
e-mail: cpvyasar@engmail.uwaterloo.ca

John McPhee
e-mail: mcphee@real.uwaterloo.ca

Stephen Birkett
e-mail: sbirkett@real.uwaterloo.ca

Systems Design Engineeering,
University of Waterloo,
Waterloo, ON, N2L 3G1, Canada

In this work, we discuss the limitations of the existing collocation-based coefficient of restitution method for simulating impacts in continuous systems. We propose a new method for modeling the impact dynamics of continuous systems based on the unit impulse response. The developed method allows one to relate modal velocity initial conditions before and after impact without requiring the integration of the system equations of motion during impact. The proposed method has been used to model the impact of a pinned-pinned beam with a rigid obstacle. Numerical simulations are presented to illustrate the inability of the collocation-based coefficient of restitution method to predict an accurate and energy-consistent response. We also compare the results obtained by unit impulse-based coefficient of restitution method with a penalty approach.
[DOI: 10.1115/1.3173667]

1 Introduction

Many mechanical systems are subjected to impact loading, either due to their functionality (such as musical instruments, impact dampers, impact hammers, and sports equipment) or due to undesirable phenomena (such as clearance in joints due to wear and rotor-stator impact in rotating machinery). In situations where the components of the system can be approximated as rigid bodies or multi-degree-of freedom vibratory systems, the impact can be successfully modeled using approaches based on the coefficient of restitution (CoR), as described in classical texts [1–3]. In CoR-based modeling, the impact is assumed to occur in an infinitesimal amount of time; thus, the wave propagation effects during the impact are neglected. An algebraic relation obtained from an energy/momentum balance is used to obtain the post-impact states of the mechanical system given the pre-impact states.

Another approach for simulating impact is local compliance modeling, which involves representing local deformations during impact with linear or nonlinear spring-damper combinations [4–6]. This approach requires the integration of the equations of motion during the impact phase. While both the CoR and local compliance approaches are widely used in the simulation of multibody system dynamics, the local compliance approach has been a popular choice when modeling impact on flexible structures as it accounts for the vibratory behavior during and after impact. A representative selection of works using this approach can be found in Refs. [7–16].

Despite the success of modeling short-duration impacts in rigid and lumped-parameter vibro-impacting systems using CoR, the extension of CoR-based modeling to structural systems has received little attention, especially when combined with modal discretization. The only work along these lines was done by Wagg and Bishop [17]. Two assumptions were made in this work:

(1) The configuration of the system does not change during the impact, in accordance with the conventional rigid body CoR approach; and
(2) The velocity field of the structure changes only at the impacting point according to the CoR method, setting up a non-smooth velocity field after impact.

Using the above assumptions, Wagg and Bishop [17] defined a modal form of CoR that relates the post-impact modal velocities to the pre-impact modal velocities. The modal form of CoR requires selecting $N-1$ locations (the collocation points) on the beam for an N-mode approximation at which the velocities are assumed to be the same before and after the impact. In doing so, the authors have approximated the assumed non-smooth post-impact velocity distribution of the beam using a function (the collocation function), which is a linear combination of N-mode shapes. The coefficients of the collocation function are obtained by equating it to the corresponding non-smooth function at the collocation and impact points.

In this work, we discuss the shortcomings of the method proposed in Ref. [17], including the fact that it can lead to artificial energy input into the mechanical structure under certain combinations of collocation points. We propose a new energy-consistent method for obtaining post-impact modal initial conditions using the unit impulse response. The developed method does not require choosing collocation points. We also compare our results with the local compliance method using very high contact stiffness, which approximately corresponds to the case of near-rigid collisions. A simply-supported vibro-impacting beam, discretized using the Galerkin approximation, is considered to demonstrate the proposed method.

2 Mathematical Modeling

The schematic of the physical system being modeled as well as the related nomenclature are shown in Fig. 1. The system consists of a pinned-pinned beam excited harmonically at location x_f by a force $F\sin(\omega t)$. The motion of the beam at location x_i is constrained by a rigid stop.

The equation governing the dynamics of the beam, excluding the event of impact and assuming Euler–Bernoulli beam theory, is given by the following:

$$EI\frac{\partial^4 w}{\partial x^4}+\rho A\frac{\partial^2 w}{\partial t^2}=F\sin(\omega t)\delta(x-x_f),\quad w(x_i,t)\le D \tag{1}$$

[1]Corresponding author.

Contributed by the Applied Mechanics Division of ASME for publication in the JOURNAL OF APPLIED MECHANICS. Manuscript received July 4, 2008; final manuscript received April 13, 2009; published online December 10, 2009. Review conducted by Prof. Sridhar Krishnaswamy.

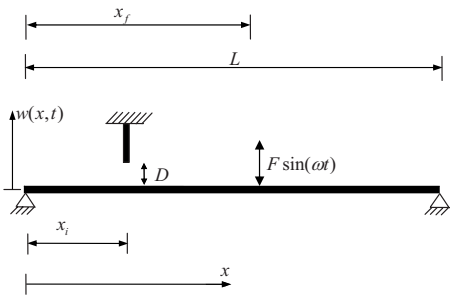

Fig. 1 Schematic of the physical system

where E is the Young's modulus, I is the area moment of inertia, ρ is the density, A is the cross-sectional area, δ is Dirac's function, and t is the time. The boundary conditions for pinned-pinned supports are as follows:

$$w(0,t) = w(L,t) = 0 \quad \text{and} \quad \frac{\partial^2 w(0,t)}{\partial x^2} = \frac{\partial^2 w(L,t)}{\partial x^2} = 0 \tag{2}$$

We introduce the following dimensionless parameters into the equation of motion:

$$x^* = \frac{x}{L}, \quad w^* = \frac{w}{D}, \quad t^* = t\sqrt{\frac{EI}{\rho AL^4}}, \quad \omega^* = \omega\sqrt{\frac{\rho AL^4}{EI}}, \quad F^* = \frac{FL^4}{EID} \tag{3}$$

The equation of motion, after dropping the asterisks for simplicity, then becomes

$$\frac{\partial^4 w}{\partial x^4} + \frac{\partial^2 w}{\partial t^2} = F\sin(\omega t)\delta(x - x_f), \quad w(x_i,t) \leq 1 \tag{4}$$

with the following boundary conditions:

$$w(0,t) = w(1,t) = 0 \quad \text{and} \quad \frac{\partial^2 w(0,t)}{\partial x^2} = \frac{\partial^2 w(1,t)}{\partial x^2} = 0 \tag{5}$$

Two further initial conditions are required:

$$w(x,0) = w_0(x) \quad \text{and} \quad \dot{w}(x,0) = \dot{w}_0(x) \tag{6}$$

A solution to Eq. (4) is assumed to be of the following form:

$$w(x,t) = \sum_{j=1}^{\infty} \phi_j(x)\eta_j(t) \tag{7}$$

where $\phi_j(x)$ and $\eta_j(t)$ corresponds to the jth mass-normalized mode shape and the corresponding modal coordinate for the beam. Substituting the above form of solution into Eq. (4) and applying the principle of orthogonality results in an infinite number of ordinary differential equations (ODEs). Truncating the system to N modes gives the following finite set of ODEs:

$$\ddot{\eta}_j(t) + \omega_j^2\eta_j(t) = \phi_j(x_f)F\sin(\omega t), \quad j = 1,2,\ldots,N \tag{8}$$

where ω_j are the natural frequencies of the beam. The modal initial conditions can be obtained as follows:

$$\eta_j(0) = \int_0^1 w(x,0)\phi_j(x)dx \quad \text{and} \quad \dot{\eta}_j(0) = \int_0^1 \dot{w}(x,0)\phi_j(x)dx \tag{9}$$

2.1 Impact Modeling. Once the system parameters have been specified, Eq. (8) can be numerically integrated until the impact. At the impact event, we have information about the pre-impact displacement and velocity distribution of the beam, which are $w(x,t_-)$ and $\dot{w}(x,t_-)$, where t_- is the time at which impact occurs. The objective is to relate the pre-impact displacement and velocity distributions to the post-impact distributions. In rigid-body problems involving translation, if the velocity of one point is known, then the velocities of all other points on the rigid body can be easily derived. With continuous systems, however we must predict the post-impact velocity distribution, $\dot{w}(x,t_+)$, given only a post-impact velocity at the impact location, $\dot{w}(x_i,t_+)$. At the instant of impact, it is assumed that the configuration of the system does not change, as was assumed in Ref. [17]:

$$w(x,t_+) = w(x,t_-) \tag{10}$$

The corresponding modal post-impact displacement initial conditions are

$$\eta_j(t_+) = \eta_j(t_-), \quad j = 1,2,\ldots N \tag{11}$$

The velocity of the beam at the impact location changes according to the following classical CoR rule:

$$\dot{w}(x_i,t_+) = -R\dot{w}(x_i,t_-) \tag{12}$$

where R is the coefficient of restitution. In addition to Eq. (12), the pre-impact velocity distribution $\dot{w}(x,t_-)$ is also known. Now we must obtain the post-impact velocity distribution, $\dot{w}(x,t_+)$, satisfying Eq. (12). The method proposed in Ref. [17] for obtaining the post-impact velocity distribution and the corresponding modal velocity initial condition proceeds as follows. First, Eq. (12) can be written as follows:

$$\sum_{j=1}^{N} \phi_j(x_i)\dot{\eta}_j(t_+) = -R\sum_{j=1}^{N} \phi_j(x_i)\dot{\eta}_j(t_-) \tag{13}$$

In order to solve for the post-impact modal velocity initial conditions, we need $N-1$ additional equations, which can be obtained from the assumption that the velocity of the beam remains the same before and after impact at all points except for the impact location. Selecting $N-1$ arbitrary points (collocation points), we have the following relationships:

$$\dot{w}(x_{ck},t_+) = \dot{w}(x_{ck},t_-), \quad k = 1,2,\ldots,N-1 \tag{14}$$

which can be further expressed as follows:

$$\sum_{j=1}^{N} \phi_j(x_{ck})\dot{\eta}_j(t_+) = \sum_{j=1}^{N} \phi_j(x_{ck})\dot{\eta}_j(t_-), \quad k = 1,2,\ldots,N-1 \tag{15}$$

Equations (13) and (15) can now be expressed in matrix form. As an example, we show the matrix form for a three-mode problem. Figure 2 illustrates the collocation method for obtaining the post-impact velocity distribution. In this case, we must choose two collocation points, x_{c1} and x_{c2}, as well as the impact point, x_i. The matrix equation relating the pre- and post-impact modal velocities can be written as follows:

$$\begin{Bmatrix} \dot{\eta}_1(t_+) \\ \dot{\eta}_2(t_+) \\ \dot{\eta}_3(t_+) \end{Bmatrix} = [\mathbf{\Phi}]^{-1}\begin{bmatrix} 1 & 0 & 0 \\ 0 & -R & 0 \\ 0 & 0 & 1 \end{bmatrix}[\mathbf{\Phi}]\begin{Bmatrix} \dot{\eta}_1(t_-) \\ \dot{\eta}_2(t_-) \\ \dot{\eta}_3(t_-) \end{Bmatrix}$$

where

$$[\mathbf{\Phi}] = \begin{bmatrix} \phi_1(x_{c1}) & \phi_2(x_{c1}) & \phi_3(x_{c1}) \\ \phi_1(x_i) & \phi_2(x_i) & \phi_3(x_i) \\ \phi_1(x_{c2}) & \phi_2(x_{c2}) & \phi_3(x_{c2}) \end{bmatrix} \tag{16}$$

It is clear from Eq. (16) that the post-impact modal velocities are strongly dependent on the selected collocation points and can lead to completely different vibro-impacting system dynamics. Certain choices of collocation points may also lead to the artificial input of energy into the mechanical oscillator—that is, where the predicted post-impact velocity distribution contains more energy than the pre-impact velocity distribution. In order to resolve this issue, a new method is proposed in the next section.

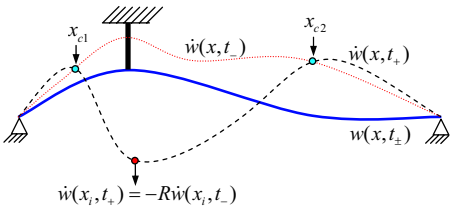

Fig. 2 Illustration of collocation method

2.2 The Impulse-Based CoR Method. Before discussing the proposed impulse-based CoR method, we revisit the idea of the unit impulse response of a continuous system. The equation of motion of a beam with a unit impulse as the forcing function, acting at the impact location x_i at time $t=t_-$, can be written as follows:

$$\frac{\partial^4 w}{\partial x^4} + \frac{\partial^2 w}{\partial t^2} = \delta(x - x_i)\,\delta(t - t_-) \tag{17}$$

which has the solution

$$w(x,t) = \sum_{j=1}^{N} \phi_j(x) \frac{\phi_j(x_i)}{\omega_j} \sin(\omega_j(t - t_-)), \quad t > t_- \tag{18}$$

and the velocity response

$$\dot{w}(x,t) = \sum_{j=1}^{N} \phi_j(x)\phi_j(x_i)\cos(\omega_j(t - t_-)), \quad t > t_- \tag{19}$$

Immediately after the application of impact (i.e., when $t=t_+$), the system has the following velocity distribution

$$\dot{w}(x,t) = \dot{U}(x,t_+) = \sum_{j=1}^{N} \phi_j(x)\phi_j(x_i) \tag{20}$$

where $\dot{U}(x,t_+)$ is the velocity distribution of the continuous structure due to a unit impulse at location x_i. The magnitude of the velocity at the impact location, x_i can now be written as follows:

$$\dot{U}(x_i,t_+) = \sum_{j=1}^{N} \phi_j(x_i)^2 \tag{21}$$

We now discuss the impulse-based CoR method. As shown in Fig. 3, we attempt to find the nondimensional impulse P that must be applied to the continuous system at the event of impact so as to obtain the post-impact velocity at the location of impact described by Eq. (12). We make use of the velocity distribution of the beam due to a unit impulse at the impact location. The calculated impulse P should generate the same initial conditions as the unit impulse, except that it has a different magnitude with a scaling factor of P.

The velocity at the impact location due to an impulse P, when added to the pre-impact velocity at the impact location, should result in the post-impact velocity at the impact location:

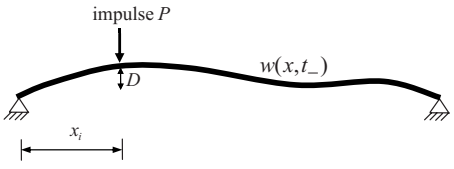

Fig. 3 Impact modeled using finite impulse

$$\dot{w}(x_i,t_-) + P\dot{U}(x_i,t_+) = \dot{w}(x_i,t_+) \tag{22}$$

In Eq. (22), the post-impact velocity $\dot{w}(x_i,t_+)$ can be expressed in terms of the pre-impact velocity using Eq. (12); thus Eq. (22) now becomes

$$\dot{w}(x_i,t_-) + P\dot{U}(x_i,t_+) = -R\dot{w}(x_i,t_-) \tag{23}$$

Rearranging Eq. (23), the magnitude of the impulse can be obtained as follows:

$$P = -(R+1)\frac{\dot{w}(x_i,t_-)}{\dot{U}(x_i,t_+)} \tag{24}$$

The post-impact velocity distribution $\dot{w}(x,t_+)$ can be obtained by superimposing the velocity distribution due to impulse P at time t_- on the pre-impact velocity distribution $\dot{w}(x,t_-)$:

$$\dot{w}(x,t_+) = \dot{w}(x,t_-) - (R+1)\frac{\dot{w}(x_i,t_-)}{\dot{U}(x_i,t_+)}\dot{U}(x,t_+) \tag{25}$$

Multiplying both sides of Eq. (25) with modal functions and integrating over the domain results in the following:

$$\dot{\eta}_j(t_+) = \dot{\eta}_j(t_-) - (R+1)\frac{\dot{w}(x_i,t_-)}{\dot{U}(x_i,t_+)}\phi_j(x_i) \tag{26}$$

Equation (26) relates the pre-impact and post-impact modal initial conditions without the need to choose collocation points.

3 Results and Discussion

CoR-based modeling is a limiting case of the local compliance approach where the stiffness of the obstacle reaches infinity. We therefore compare numerical simulations obtained by the proposed impulse-based CoR method with those from a penalty approach [7], in which the obstacle is modeled as a linear spring with very high stiffness. Now we briefly describe the penalty approach. The dimensionless equation of motion of a beam when modeled using the penalty approach is of the following form:

$$\frac{\partial^4 w}{\partial x^4} + \frac{\partial^2 w}{\partial t^2} = -F_{\text{contact}} + F\,\sin(\omega t)\,\delta(x - x_f) \tag{27}$$

where the contact force F_{contact} is represented as

$$F_{\text{contact}} = \begin{cases} K[w(x_i,t) - 1] & w(x_i,t) \geq 1 \\ 0 & w(x_i,t) < 1 \end{cases} \tag{28}$$

The boundary conditions and initial conditions are given by Eqs. (5) and (6). When the beam penetrates into the obstacle, a contact force is generated as described by Eq. (28). If the penalty parameter (contact stiffness K) is chosen sufficiently high, the penetration of the beam will be very small and will approach zero as K

Table 1 Dimensionless parameters used in simulation

Physical parameter	Quantity
Penalty stiffness	1×10^{12}
Impact location (x_i)	0.5
Coefficient of restitution	1

Table 2 Parameters for collocation method

No. of modes	Collocation points
4	CP1=[0.2,0.3,0.7]
4	CP2=[0.15,0.4,0.8]
4	CP3=[0.1,0.35,0.9]

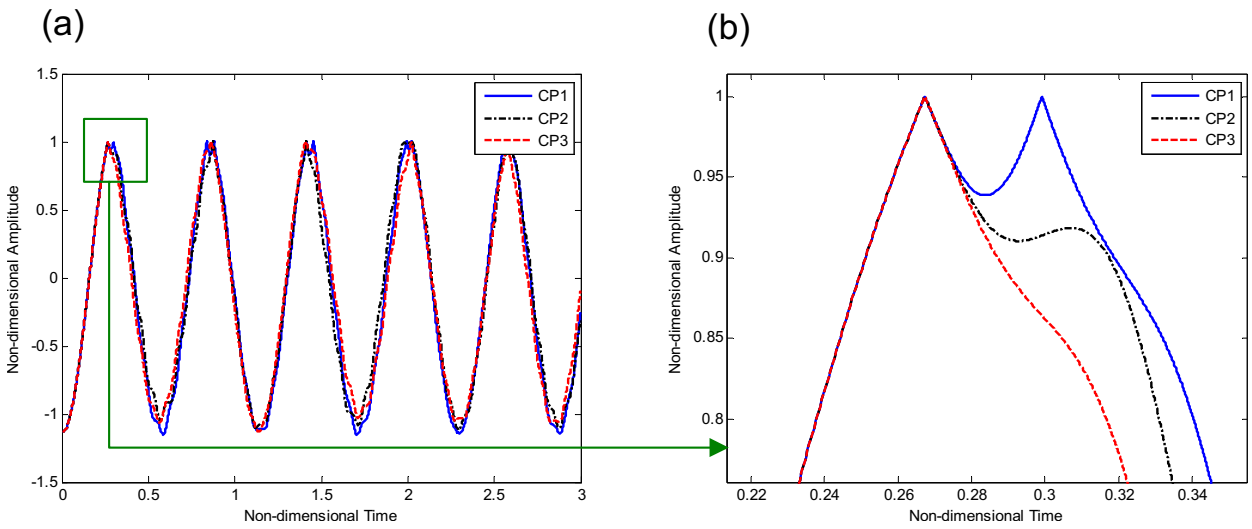

Fig. 4 Response at the impact location: (*a*) displacement and (*b*) magnified view at first impact

tends to infinity. The contact forces generated will push the beam away from the obstacle, thus simulating its impact behavior. Equation (27) along with contact force expression (Eq. (28)) were solved numerically using modal analysis combined with the force integration method [7].

Initially, we present the numerical solution for a free vibration problem and emphasize the energy-conserving nature of the formulation. The initial conditions for this particular study are as follows:

$$w(x,0) = -1.01\sin(\pi x) \quad \text{and} \quad \dot{w}(x,0) = 0 \tag{29}$$

Table 1 shows the dimensionless parameters used in the numerical simulation. We compare the four-mode solutions obtained by choosing different sets of collocation points, shown in Table 2. The modal equations given by Eq. (8) are solved in MATLAB using the numerical integrator ode45 and the built-in event detection algorithm for detecting impacts. Relative and absolute tolerances were chosen to be 10^{-9}.

Figure 4(*a*) shows the displacement of the beam at the impact location for different sets of collocation points. Figure 4(*b*) shows a magnified version of the displacement at the first impact, and clearly illustrates the dependence of the response on the selected collocation points. This dependence is also confirmed in Figs. 5 and 6, which show the velocity and phase plot at the impact location.

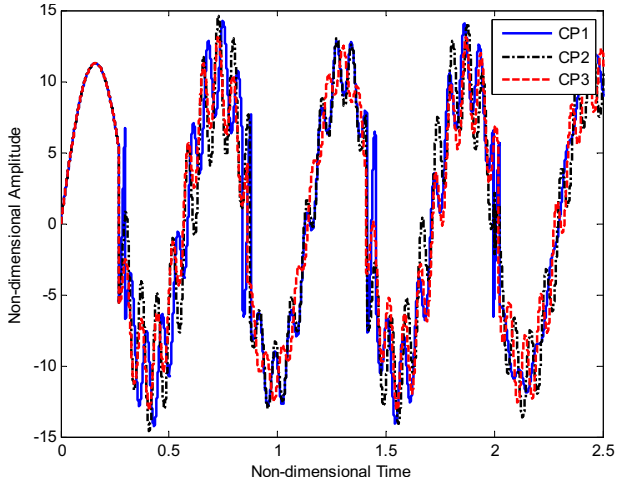

Fig. 5 Velocity at impact location

Figure 7 clearly shows that the energy of the mechanical system is increasing. It should be noted that, since the current problem is a free vibration problem with CoR equal to 1, the energy in the system should be conserved.

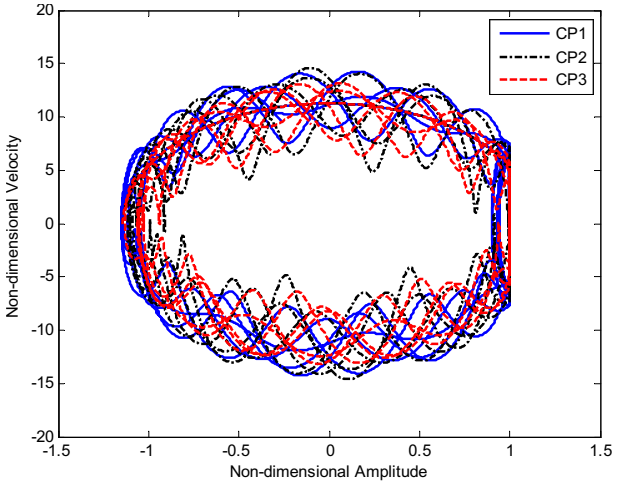

Fig. 6 Phase plot at impact location

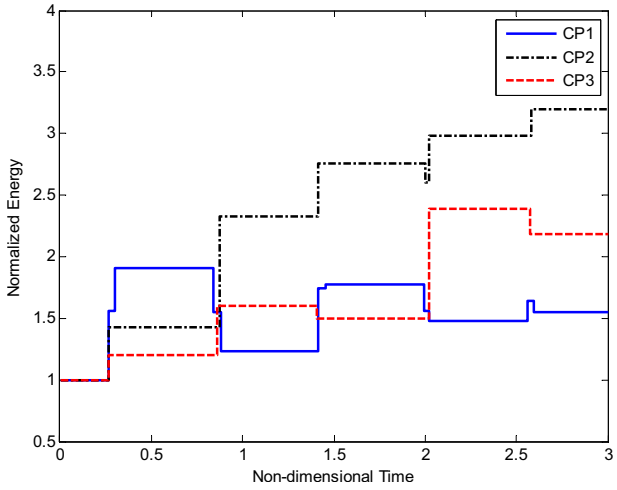

Fig. 7 Energy of the mechanical system

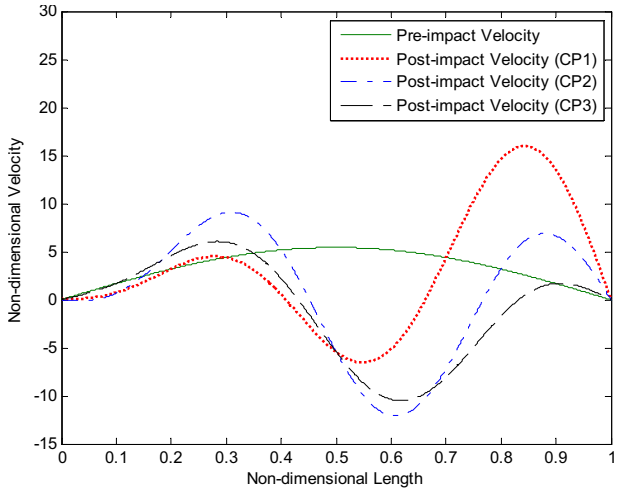

Fig. 8 Pre- and post-impact velocity distributions

The lack of energy conservation can be explained by Fig. 8, which shows the pre- and post-impact velocity distributions at the first impact for different sets of collocation points. It can be seen that the post-impact velocity distributions are different for different selections of collocation points. Since it is assumed that the displacement configuration remains the same before and after impact, the strain energy cannot be altered and any incorrect predictions of post-impact initial conditions can lead to spurious energy input. Equation (15) strongly enforces that the pre- and post-impact velocities match at the collocation points, and relates velocities at the impact location, as given by Eq. (12), but we have no control over the velocity at other points.

Now we show the results obtained for a four-mode problem using the impulse-based CoR method proposed in this paper. Figures 9(*a*) and 9(*b*) show the displacements at the impact location obtained for free and forced vibration problems using both the impulse-based CoR and the penalty method. The dimensionless parameters for forcing function amplitude, location, and frequency are shown in Table 3. The forcing function frequency is chosen to be the first natural frequency of the beam. It can be clearly seen that the solutions agree exactly. This fact is further illustrated in Figs. 10 and 11, which show the velocity and phase portrait at the impact location.

Figure 12 shows the energy in the mechanical system for the free vibration problem, illustrating that the impulse-based CoR approach with CoR=1 and the penalty approach formulation both preserve the energy of the mechanical system. As the coefficient of restitution is decreased, the beam loses energy at every impact. Interestingly, with CoR=0.5 the beam settles at an energy level that is higher than that obtained with CoR=0.8. The total energy lost is a function of number of impacts, the pre-impact velocity, and the CoR. More energy is lost at each impact for CoR=0.5 for same pre-impact velocity (first impact), while more impacts occur for CoR=0.8 during the current simulation time.

Table 3 Dimensionless parameters for forcing function

Physical parameter	Quantity
Amplitude of forcing function (F)	72
Location of forcing function (x_f)	0.5
Frequency of forcing function ($\omega=\omega_1$)	π^2

The impulse-based CoR approach has an advantage over the penalty approach in terms of computational efficiency and provides identical results. A comparison of normalized computation times for the forced response problem using the impulse-based CoR and penalty approach is shown in Fig. 13. It is evident from the graph that the computational efficiency of the impulse-based CoR method provides increasing benefit as the number of modes considered in the problem is increased. For example, the penalty method is nine times slower than the impulse-based CoR approach when nine modes are considered in the analysis. The proposed method can be used to successfully simulate the impact behavior at a much lower computational cost compared to the penalty approach, where a large number of numerical parametric studies are to be performed to characterize the behavior of the vibro-impacting systems. The developed method can also be incorporated into finite element codes if the analysis is carried out in the modal domain and a prior knowledge of the response of the structure due to unit impulse at the impact location is known.

4 Conclusions

It has been shown that the collocation-based CoR approach can introduce energy into the mechanical system for certain selections of collocation points. The new impulse-based CoR approach presented herein is energy consistent and predicts a response that is very close to that obtained using the penalty approach. Moreover, the impulse-based CoR approach has been seen to provide increased computational efficiency over the penalty approach as the number of modes considered in the analysis was increased. Al-

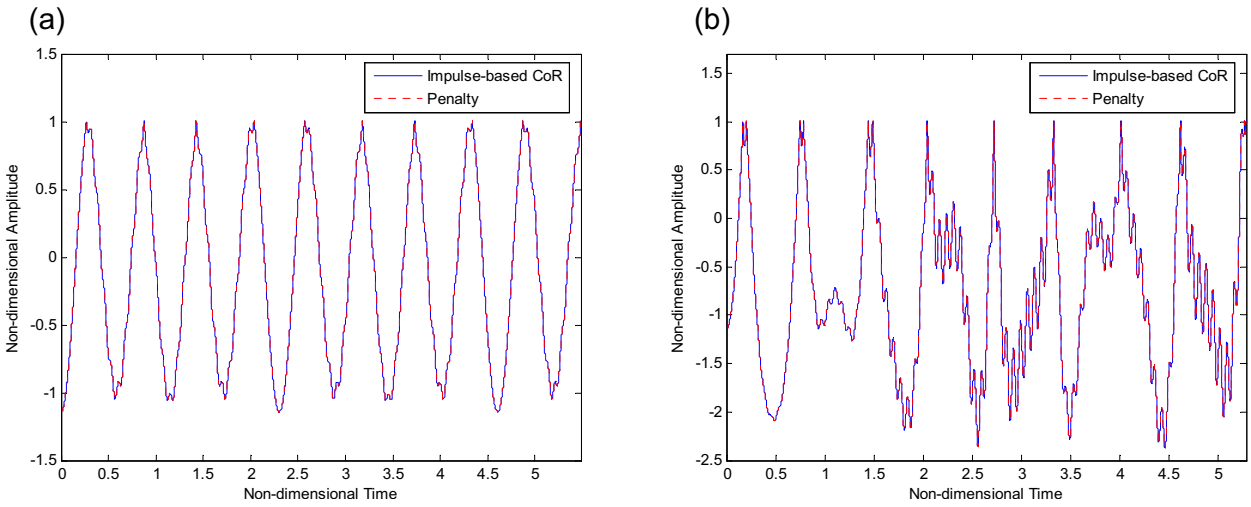

Fig. 9 Displacement at the impact location: (*a*) free vibration and (*b*) forced vibration

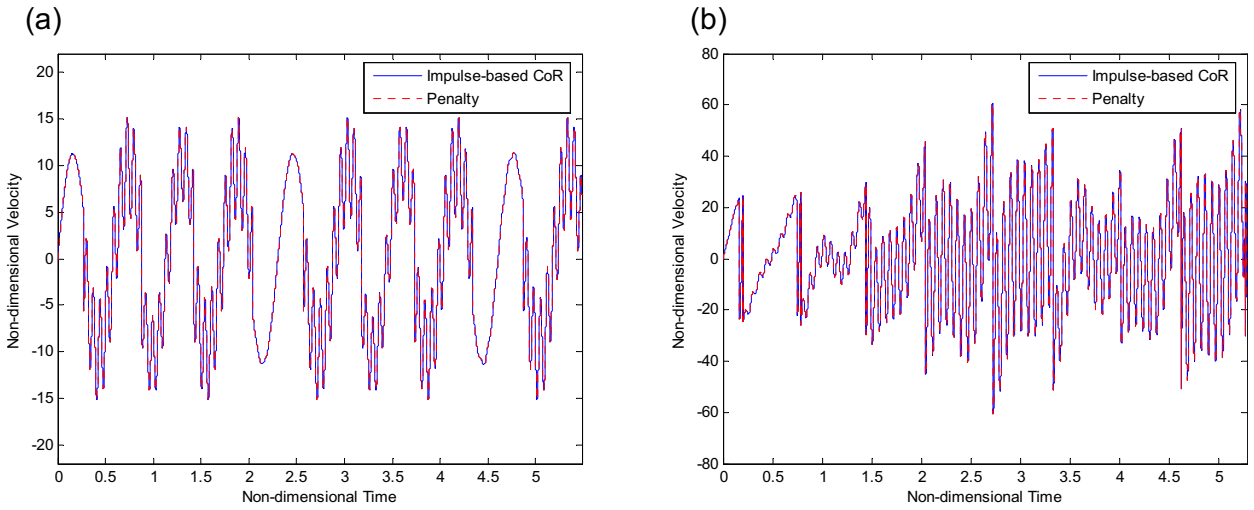

Fig. 10 Velocity at the impact location: (*a*) free vibration and (*b*) forced vibration

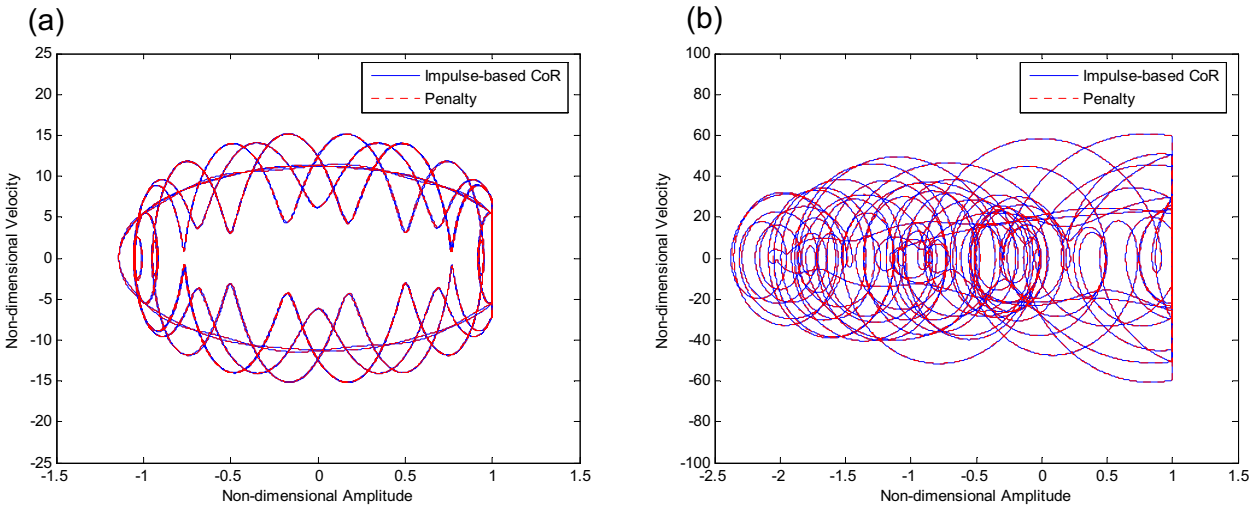

Fig. 11 Phase plot at the impact location: (*a*) free vibration and (*b*) forced vibration

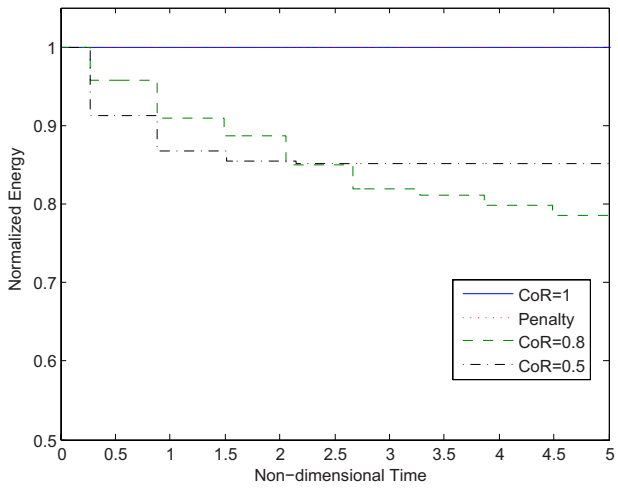

Fig. 12 Energy in the mechanical system in free vibration

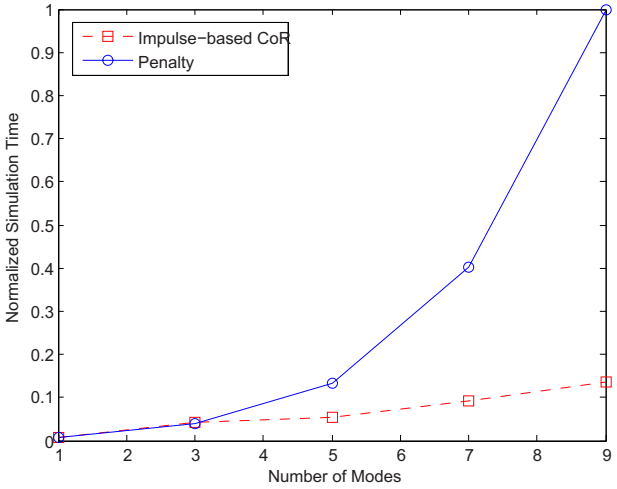

Fig. 13 Comparison of computational efficiency

though the impulse-based CoR method has only been applied to a vibro-impacting beam, the method can be applied to any continuous mechanical system that can be discretized using modal-based methods.

Acknowledgment

The lead author expresses his thanks to Sukhpreet Sandhu and Dr. Kingshook Bhattacharyya for the many interesting discussions during the course of this study. Funding of this research by the Natural Sciences and Engineering Research Council of Canada is gratefully acknowledged.

References

[1] Goldsmith, W., 1960, *Impact*, Arnold, London.
[2] Brach, R. M., 1991, *Mechanical Impact Dynamics: Rigid Body Collisions*, Wiley, New York.
[3] Stronge, W. J., 2000, *Impact Mechanics*, Cambridge University, Cambridge.
[4] Hunt, K. H., and Crossley, F. R. E., 1975, "Coefficient of Restitution Interpreted as Damping in Vibroimpact," ASME J. Appl. Mech., **42**, pp. 440–445.
[5] Lankarani, H. M., and Nikravesh, P. E., 2004, "Continuous Contact Force Models for Impact Analysis in Multibody Systems," Nonlinear Dyn., **5**, pp. 193–207.
[6] Gonthier, Y., McPhee, J., Lange, C., and Piedboeuf, J. C., 2004, "A Regularized Contact Model With Asymmetric Damping and Dwell-Time Dependent Friction," Multibody Syst. Dyn., **11**, pp. 209–233.
[7] Tsai, H. C., and Wu, M. K., 1996, "Methods to Compute Dynamic Response of a Cantilever With a Stop to Limit Motion," Comput. Struc., **58**, pp. 859–867.
[8] Wang, C., and Kim, J., 1996, "New Analysis Method for a Thin Beam Impacting Against a Stop Based on the Full Continuous Model," J. Sound Vib., **191**, pp. 809–823.
[9] Wang, C., and Kim, J., 1997, "The Dynamic Analysis of a Thin Beam Impacting Against a Stop of General Three-Dimensional Geometry," J. Sound Vib., **203**, pp. 237–249.
[10] de Vorst, E. L. B. V., Heertjes, M. F., Campen, D. H. V., de Kraker, A., and Fey, R. H. B., 1998, "Experimental and Numerical Analysis of the Steady State Behaviour of a Beam System With Impact," J. Sound Vib., **212**, pp. 321–336.
[11] Metallidis, P., and Natsiavas, S., 2000, "Vibration of a Continuous System With Clearance and Motion Constraints," Int. J. Non-Linear Mech., **35**, pp. 675–690.
[12] Knudsen, J., and Massih, A. R., 2000, "Vibro-Impact Dynamics of a Periodically Forced Beam," ASME J. Pressure Vessel Technol., **122**, pp. 210–221.
[13] Turner, J. A., 2004, "Nonlinear Vibrations of a Beam With Cantilever-Hertzian Contact Boundary Conditions," J. Sound Vib., **275**, pp. 177–191.
[14] Bao, Z., Goyal, S., Leu, L. J., and Mukherjee, S., 2004, "The Role of Beam Exibility and Ground Contact Model in the Clattering of Deformable Beams," ASME J. Dyn. Syst., Meas., Control, **126**, pp. 421–425.
[15] Lin, W., Qiao, N., and Yuying, H., 2006, "Bifurcations and Chaos in a Forced Cantilever System With Impacts," J. Sound Vib., **296**, pp. 1068–1078.
[16] Ervina, E. K., and Wickert, J. A., 2007, "Repetitive Impact Response of a Beam Structure Subjected to Harmonic Base Excitation," J. Sound Vib., **307**, pp. 2–19.
[17] Wagg, D. J., and Bishop, S. R., 2002, "Application of Non-smooth Modelling Techniques to the Dynamics of Flexible Impacting Beam," J. Sound Vib., **256**, pp. 803–820.